

Application of 3D Euler deconvolution of aeromagnetic data and pseudogravity transforms in mineral exploration: a case study of the pegmatite-rich zones of Lafiagi, Central Nigeria

A.K. Olawuyi¹ · B.D. Ako² · G.O. Omosuyi² · A.O. Adelusi²

Received: 21 August 2015 / Accepted: 5 October 2016
© Saudi Society for Geosciences 2016

Abstract Structural evaluation of the pegmatite-rich zones in a part of Lafiagi (Sheet 203), Central Nigeria, was carried out. It was aimed at identification of the structures responsible for the rich mineralization of the area. This work involved the qualitative and quantitative analysis of aeromagnetic data and pseudogravity transforms by using Oasis Montaj™ software. The 3D Euler deconvolution results from acquired aeromagnetic data and pseudogravity transforms augmented with geological information obtained from reliable sources were employed in the structural interpretation work. The results have shown that the abundance of 2D and 3D structures that are commonly associated with gemstones and precious minerals explain why the study area is rich in mineral deposits.

Keywords Pegmatite-rich zones · Mineralization · Deconvolution · Structures · Aeromagnetic and pseudogravity

Introduction

The study area covers a part of Lafiagi (Sheet 203) in the Nigerian topographical map. It is situated at the transition environment between the Nupe Basin and the southwestern Nigerian basement complex. It is bounded by latitudes 8° 40' and 8° 51' N and longitude 5° 00' and 5° 23' E, covering an area of 896.6 km² (Fig. 1a, b). The Nupe Basin is a NW–SE trending embayment (Fig. 1a) perpendicular to the main axis

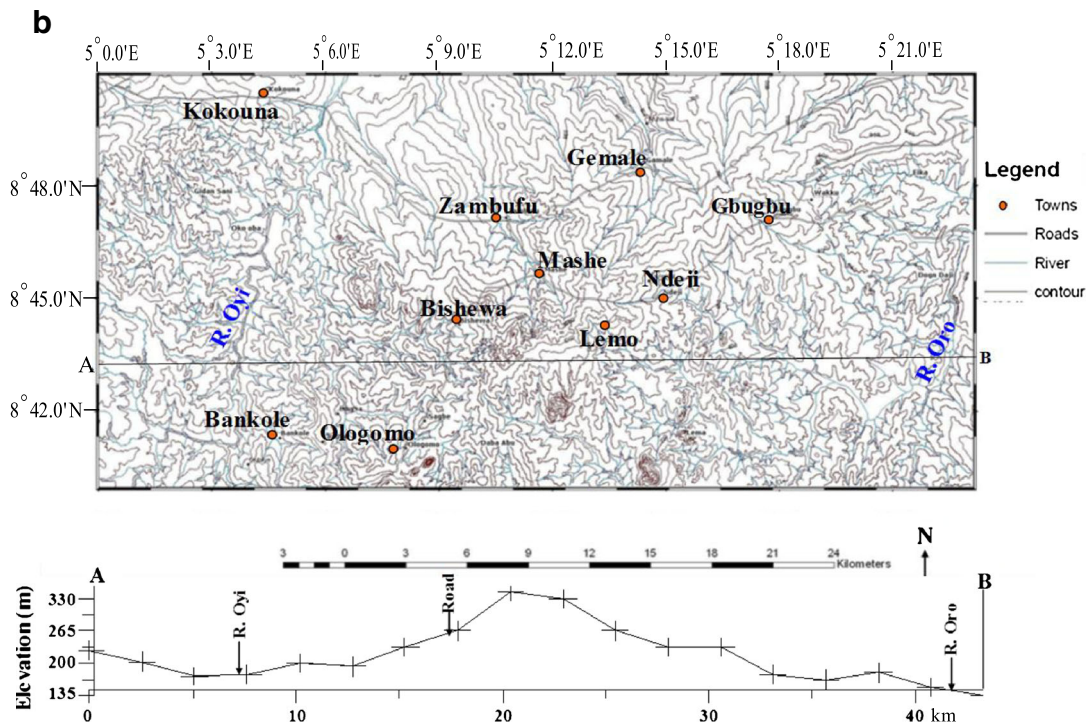
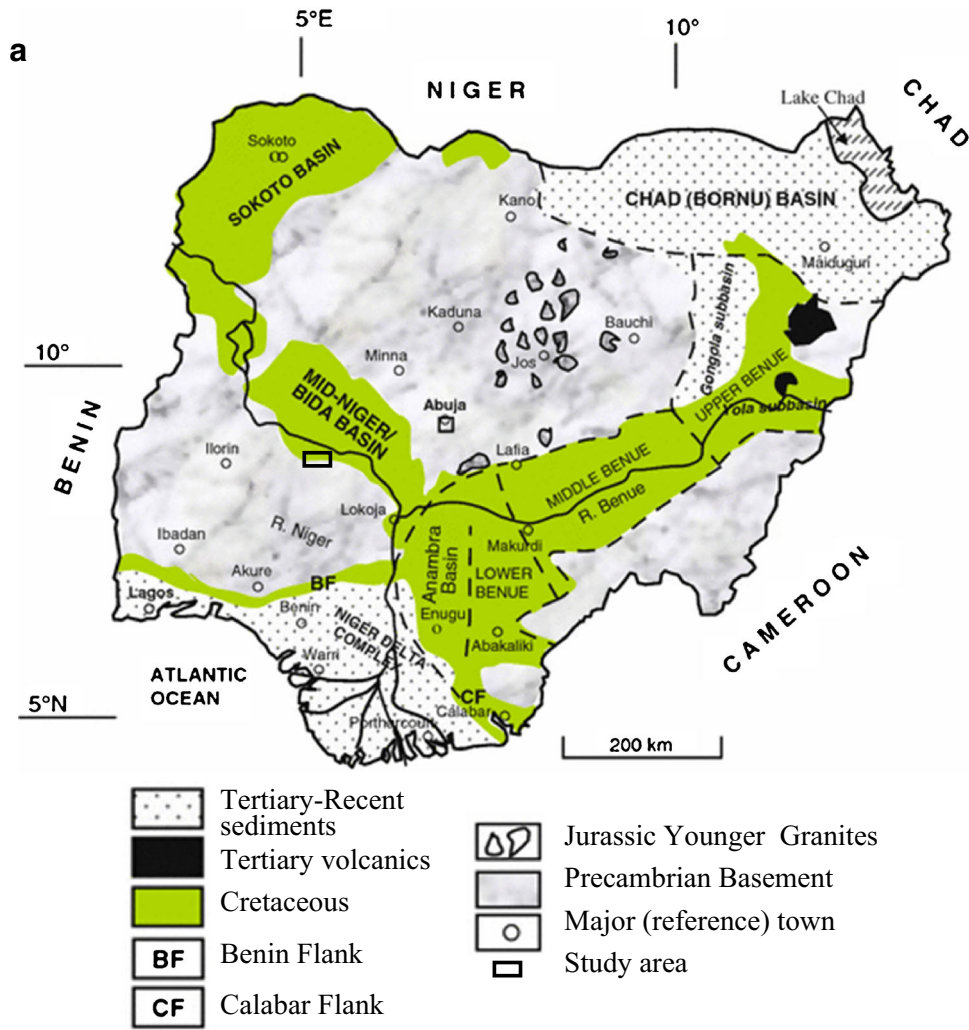
of the Benue Trough and the Niger Delta Basin of Nigeria. It is frequently regarded as the northwestern extension of the Anambra Basin, both of which were major depocenters during the transgressive cycle of Southern Nigeria in the Late Cretaceous times (Murat 1972). It has rocks of sedimentary basin flanked by the basement complex rocks of southwestern and north central Nigeria. Evidence from the eastern and northern margins of the West African craton indicates that the Pan-African belt evolved by plate tectonic processes which involved the collision between the passive continental margins of the West African craton and the active continental margin (Pharusian belt) of the Tuareg shield about 600 Ma ago (Leblanc 1981; Black et al. 1979; Caby et al. 1981). The collision at the plate margin is believed to have led to the reactivation of the internal region of the belt. The Nigerian basement complex lies at the reactivated part of the belt. The Pan-African in Nigeria was followed by conjugate strike slip fault systems which average in the NE–SW and NW–SE direction and which show dextral and sinistral sense of displacement which cut across the earlier Pan-African structures (Wright 1976; Ball 1980).

A contact or transition zone exists between the basement and sedimentary environments in the study area (Fig. 2), and the area is also rich in mineral deposits and has generated a lot of interests because of the considerable mining activities that is taking place there. The mining of rare metals and gemstone-bearing pegmatite is well known in the Gbugbu, Lema, and Bishewa communities (Garba 2011). A central positive gravity anomalies flanked by negative anomalies have been confirmed for this basin as shown for the adjacent Benue Trough and typical of rift structures (Ojo 1984; Ojo and Ajakaiye 1989). The basin has also been confirmed to be bounded by a system of linear faults trending NW–SE, by using geophysical data (Kogbe et al. 1983). In this research, a part of Lafiagi (Sheet 203) which includes the transition zone between a part

✉ A.K. Olawuyi
gideonola2001@yahoo.com

¹ Department of Geophysics, University of Ilorin, Ilorin, Nigeria

² Department of Applied Geophysics, Federal University of Technology, Akure, Nigeria



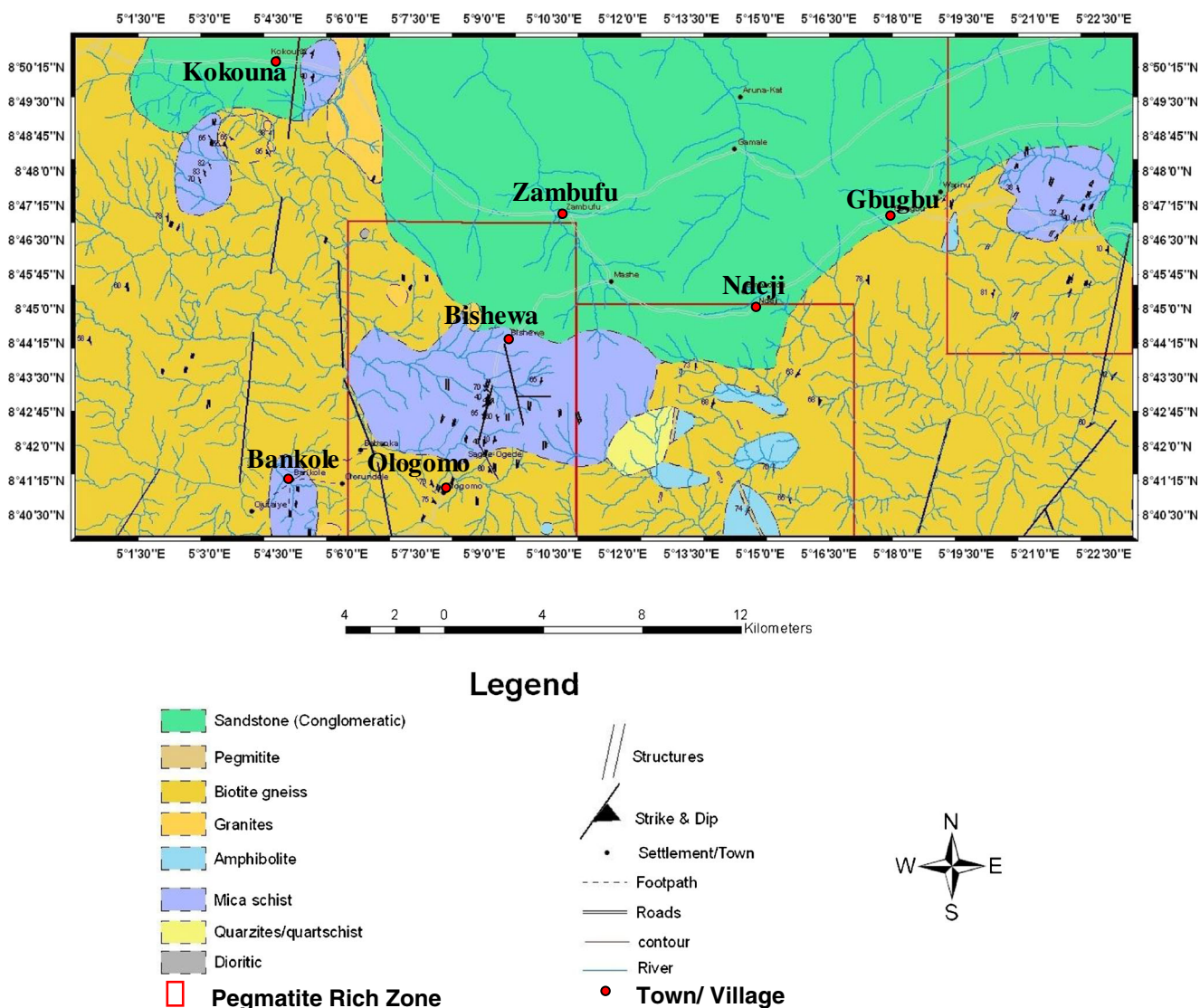


Fig. 2 Geological map of the study area (adapted from Garba 2011)

of the Nupe Basin area and the adjacent southwestern Nigeria basement complex has been mapped, its subsurface structures elucidated and the prospective mineralized zones identified.

Materials and methods

Data source and analysis

The soft copy of digital aeromagnetic data (i.e., Lafiagi aeromagnetic grid map, Sheet 203) was procured from the Nigeria Geological Survey Agency (NGSA), Abuja, Nigeria. The

survey which was aimed at mineral and groundwater development through improved geological mapping was collected at a nominal flight altitude of 80 m, flight line spacing of 500 m, and tie line spacing of 2000 m. The airborne survey data were published in the form of 0.5° by 0.5° grid maps of total magnetic intensity (TMI) on a scale of 1:100,000. The research area is a part of Lafiagi (Sheet 203) aeromagnetic map. The flight line direction was NW–SE, whereas the tie lines were NE–SW. For ease of processing, the data was stripped of a common value of 32,000 nT. This value may therefore be added to every data point to get the exact regional field. However, doing this will not change the grid in any way since the value is common to all the data points.

Data collection for this area was done in 2006, so a 2005 epoch International Geomagnetic Reference Field (IGRF) was used to calculate inclination and declination as follows:

Field strength = 33,129.9632 nT; inclination = -6.87339275; declination = -2.51357917.

◀ Fig. 1 a Geological sketch map of Nigeria showing the major geological components (basement, younger granites, and sedimentary basins) and the study area (top) (adapted from Obaje 2009). b Topographical map showing drainage and geomorphology and the elevation view along AB (bottom) (adapted from Garba 2011)

Figure 3 is the TMI map of the study area. The map emphasizes the intensities and the wavelengths of the local anomalies that reveal information on the geometry, strike, contacts between rocks, and intensities of magnetization within the study area. Several anomalies can be referred to distinct magnetic zones.

The reduction to pole (RTP) processing of Baranov and Naudy (1964) is used to remove from magnetic anomaly data the distorting effect of the varying inclination and azimuth of the magnetization vector. This process converts the magnetic field data to what the data would have looked like if the direction of magnetization had been vertical (Sharma 1997). This kind of presentation considerably improves the correlation of anomaly features with the plan view boundaries of causative geological bodies. Silva (1986) has analyzed the problem of instability in the Fourier transform method of RTP filtering at low magnetic latitudes and has developed an alternative method by using equivalent layer sources, which is effective also at low latitudes.

Poisson's relationship between gravity and magnetic fields enables the transformation of magnetic field anomalies into pseudogravity anomalies, assuming a common source. The pseudogravity anomalies are easier to analyze than magnetic anomalies, particularly for locating the edges of the anomalous source bodies. However, the transformation requires that the declination and inclination of the magnetization vector in the source bodies be known (Sharma 1997).

The reduced to equator (REDE) filter, which is a method of removing magnetic inclination effect in low magnetic latitude region, is normally used to center the peaks of magnetic

anomalies over their sources (Gilbert and Geldano 1985). In this work, the REDE and the pseudogravity filters were used for the reasons obviously stated earlier. Also, the fact that ground magnetic and gravity data could not be acquired at the same grid spacing (100 m) as the aeromagnetic data obtained from NGSA, especially because of the difficult terrain and other logistics, the best alternative for this work was the pseudogravity map generated properly from the aeromagnetic data by using Oasis montaj™ software.

The 3D Euler deconvolution method

The 3D Euler deconvolution technique is an equivalent method based on the Euler's homogeneity equation as developed by Reid et al. (1990) following Thompson's (1973) suggestion and operating on gridded magnetic data. The method is based on the concept that anomalous magnetic fields of localized structures are homogeneous function of the source coordinate and, therefore, satisfies Euler's homogeneity equation. The method operates on the data directly and provides a mathematical solution without recourse to any geological constraints. The application of Euler deconvolution has emerged as a powerful tool for direct determination of depth and probable source geometry in magnetic data interpretation (Barbosa et al. 1999). The Euler-derived interpretation requires only a little a priori knowledge about the magnetic source geometry and information about the magnetization vector (Barbosa et al. 2000).

The 3D Euler deconvolution processing routine of the Oasis Montaj™ is a semiautomatic location and depth determination software package for gridded magnetic and gravity data. The depths are displayed as a grid

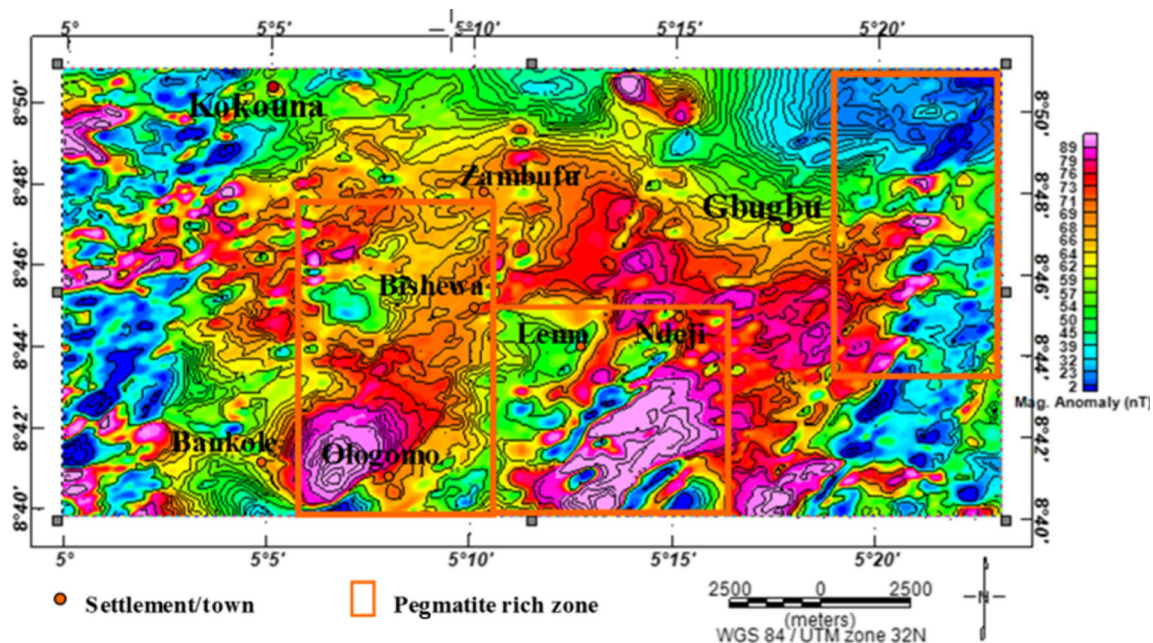


Fig. 3 Superimposition of total field aeromagnetic map (TMI) and its contour

and are based on source parameters of the following source models: contacts (faults), thin sheets (dykes), or horizontal cylinders. The structural index for gravity model is one less than that of magnetic, and the maximum for gravity is 2 (Hsu 2002).

Theory of Euler deconvolution method

Any 3D function $f(x, y, z)$ is said to be *homogeneous* of degree n if the function obeys the expression

$$f(tx, ty, tz) = t^n f(x, y, z) \quad (1)$$

From this, it can be shown that the following (known as *Euler's equation*) is also satisfied:

$$x \frac{\partial f}{\partial x} + y \frac{\partial f}{\partial y} + z \frac{\partial f}{\partial z} = nf \quad (2)$$

Considering potential field data, Euler's equation can be restated as follows (see Whitehead and Musselman 2005):

$$(x-x_0) \frac{\partial T}{\partial x} + (y-y_0) \frac{\partial T}{\partial y} + (z-z_0) \frac{\partial T}{\partial z} = N(B-T) \quad (3)$$

where (x_0, y_0, z_0) is the position of a magnetic source whose total field T is measured at (x, y, z) . The total field has a regional value of B . Note that N in this expression is equivalent to $-n$ in Euler's equation. The degree of homogeneity is non-positive because the potential field is inversely proportional to the distance raised to some power. The negative of the degree of homogeneity is defined as the structural index (SI), denoted as N in Eq. 3 (see Reid and Thurston 2014).

Thompson (1982) has shown that simple magnetic and gravity models conform to Euler's equation. The degree of homogeneity is source dependent and characterizes how fast the field decreases as a function of distance to the source (Davis and Li 2009). A magnetic point dipole corresponds to a structural index of 3, while a gravity point mass, a magnetic pole (theoretical), and a line of magnetic dipoles correspond to 1 (see Whitehead and Musselman 2005).

Results and discussions

Pattern interpretation of the aeromagnetic data and pseudogravity transforms

The REDE aeromagnetic and pseudogravity anomaly maps (Fig. 4a, b) have been divided into four distinct zones and subzones of various magnetic and pseudogravity characteristics. These include

- (i) Zone A which is characterized by low to intermediate magnetic reliefs (i.e., subzones A1 to A3; Fig. 4a) with corresponding high pseudogravity reliefs (i.e., subzones A1 to A5; Fig. 4b) in the northern part of the study area. The anomalies in this zone have amplitudes varying mostly from <23 to 58 nT and -0.0136 to 0.01230 mGal for magnetic data and pseudogravity transforms, respectively. The negative pseudogravity transforms may have resulted from the inclination and declination of the study area (inclination = -6.87339275 ; declination = -2.51357917).
- (ii) Zone B is characterized by anomalies with broad and wide extent having moderately high to very high and occasional low magnetic reliefs (i.e., subzones B1–B5; Fig. 4a) with corresponding low pseudogravity reliefs (i.e., subzones B1–B4; Fig. 4b) in the central part of the study area. "The prominent magnetic high that coincides with the position of pseudogravity low is assumed to be produced by bodies of low magnetic susceptibilities since the inclination of the ambient magnetic field in the area is close to 0° " (Likkasson and Ojo 1999). The NW–SE and NE–SW trends shown by these anomalies are characteristic of lineament features. Their amplitudes vary mostly from <52 to >93 nT and from -0.00991 to approx. 0.00112 mGal for magnetic data and pseudogravity transforms, respectively. The rocks here are composed mainly of Cretaceous sediments and a few other rocks like biotite gneiss, mica schist, quartzite/quartz schist, and Amphibolite.
- (iii) Zone C is characterized by ring strike and speckled mixture of high and low magnetic reliefs (i.e., subzones C1–C6; Fig. 4a) with corresponding moderately high to very high pseudogravity reliefs with mostly concentric patterns (i.e., subzones C1–C5; Fig. 4b). These anomalies have amplitudes of <23 to >93 nT and approx. -0.00336 to >0.01230 mGal for the magnetic data and pseudogravity transforms, respectively. This zone is associated on the geological map with biotite gneiss, mica schist, and Amphibolite.
- (iv) Zone D is characterized by a relatively low to intermediate magnetic (Fig. 4a) and pseudogravity (Fig. 4b) reliefs that are wedged to the extreme corner of the southwestern part of the study area (D1). The amplitudes range from approximately 35 to 52 nT (magnetic) and -0.0136 to -0.0580 mGal (pseudogravity).

Zone colored Euler solutions for 2D and 3D structures

The results obtained for structural indices 1.1 to 3.0 (i.e., thin prisms with large depth to sphere model; magnetic) and 0.5 to 2.0 (i.e., ribbon to sphere model; gravity) represents 2D and 3D structures (Hsu 2002). Figure 5a shows the result

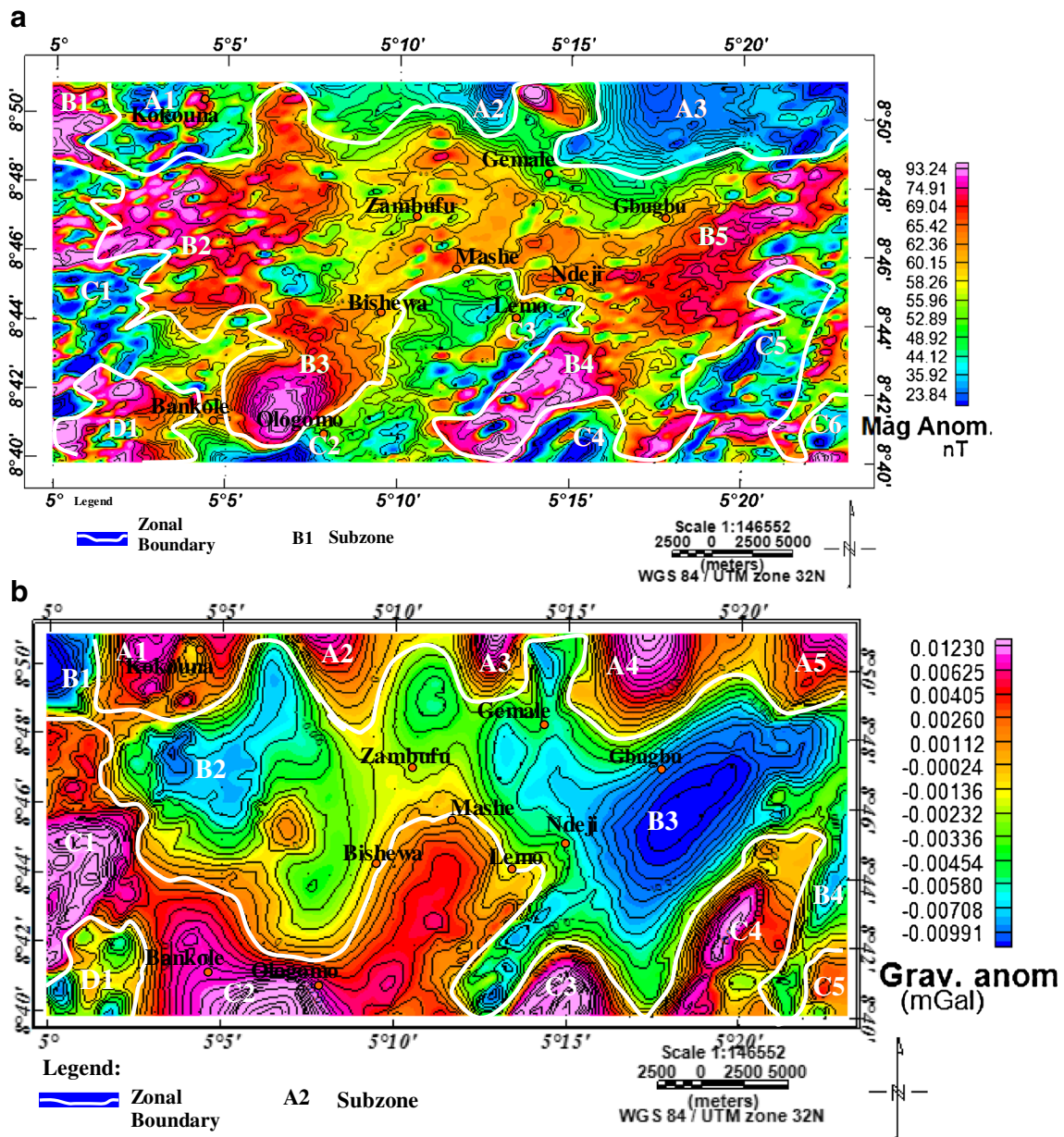
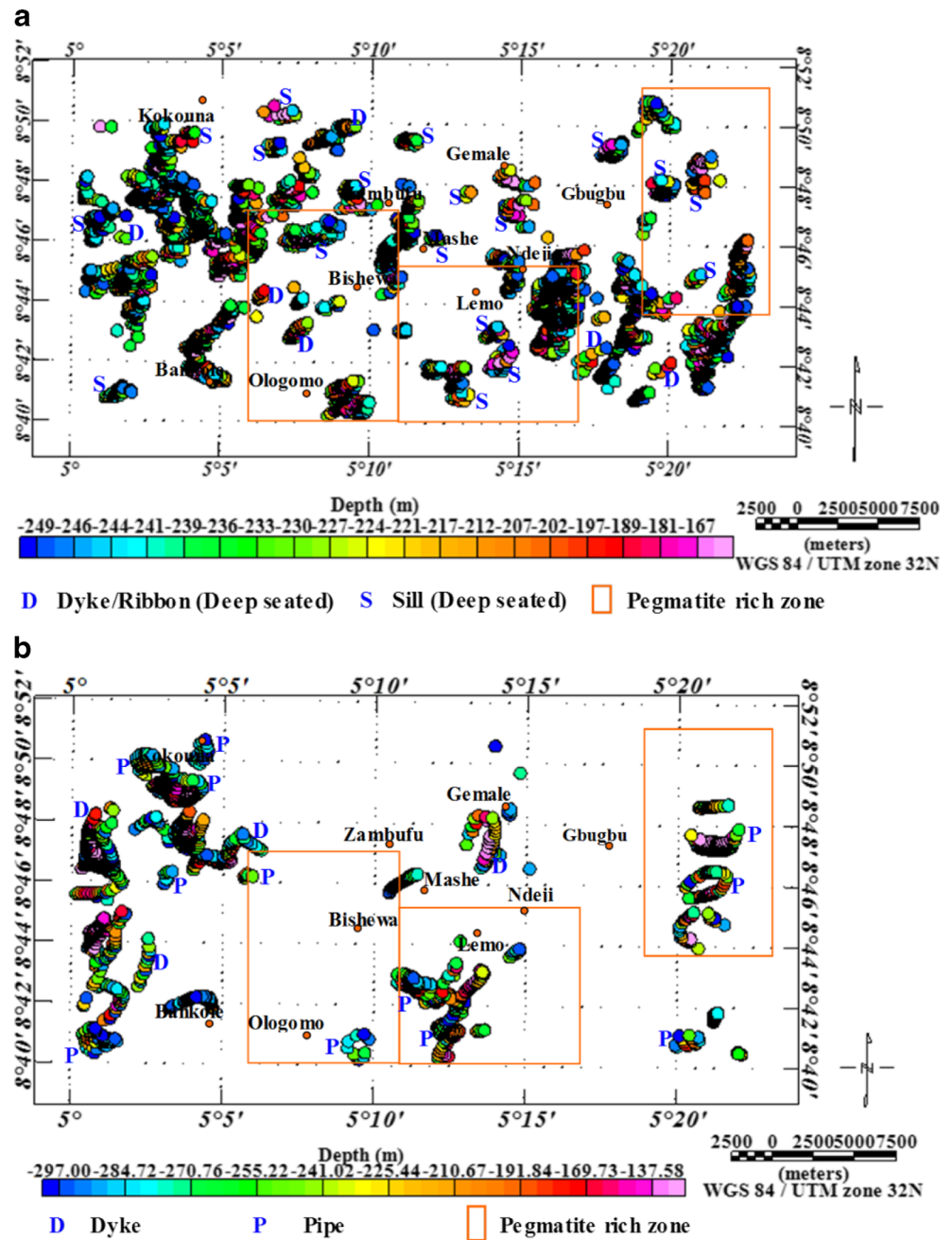


Fig. 4 **a** Total field aeromagnetic map (REDE) and its contour. **b** Pseudogravity map and its contour

obtained for structural index of 2.0 (i.e., vertical or horizontal cylinder model; magnetic) with depths ranging from 150 to 250 m. Some of these solutions which represent deep-seated dykes/ribbons and sills (intra-sedimentary or intrusives) have been shown and labeled on the map, while Fig. 5b shows the result obtained for structural index of 1.1 (i.e., pipe and dyke model; pseudogravity) with depths ranging from 139 to 297 m. The grid spacing was 100 m, and the window size of 20 was specified for Fig. 5a, b in the 3D Euler routine. The window size of 20 was achieved after some calculations and a few iterations using different window sizes. For example, in Fig. 4a, the anomalies of interest are mostly 3–6 km in width; therefore, a good estimate for

the search window size is about 6 km. Since the grid cell size is 100 m, this corresponds to about 60 grid cells; therefore, it is best to specify (20) here because it is the maximum window size specifiable in the 3D Euler deconvolution routine of Oasis montaj™ software. The iterations were based on the fact that the correct SI for a given feature will give the tightest clustering of solutions or sharpest focus of results. Whitehead and Musselman (2005) have also advised that the default window size of 20×20 in Oasis montaj™ should be adequate for typical exploration targets. The structural indices 2.0 (magnetic) and 1.1 (gravity) of 3D Euler deconvolution have been used worldwide to detect or explore for Kimberlite pipe which is well known for hosting

Fig. 5 **a** A typical aeromagnetic Euler solution map for pipe (SI = 2.0). **b** A typical pseudogravity Euler solution map for pipe (SI = 1.1)

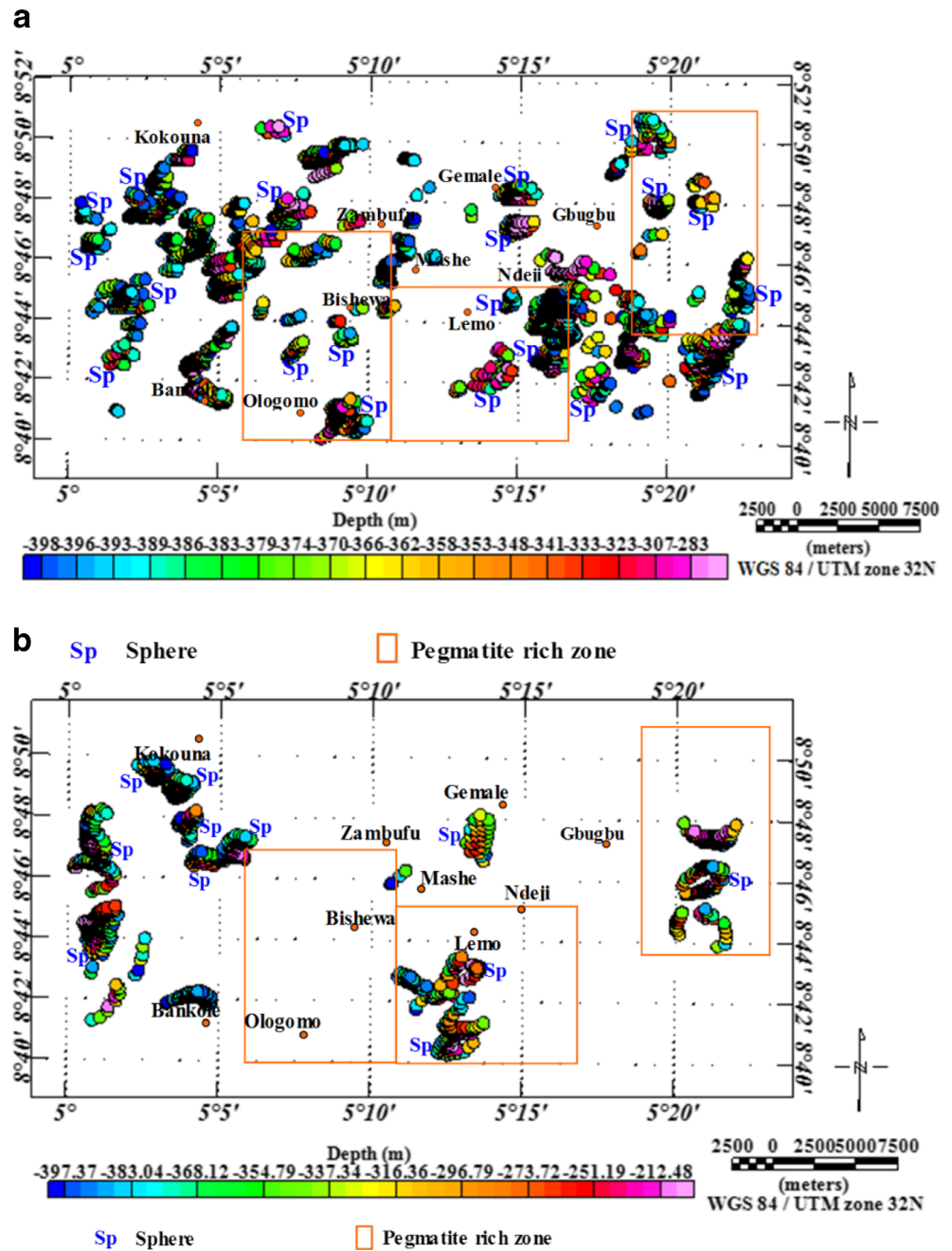


large quantity of minerals (diamonds and garnet) and rocks (peridotite and xenoliths) (Paterson et al. 1991; Yaghoobian et al. 1992).

Figure 6a shows the result obtained for structural index of 3.0 (i.e., sphere or dipole model; magnetic) with depths ranging from 250 to 400 m, while Fig. 6b shows the result obtained for structural index of 2.0 (i.e., sphere or dipole model; pseudogravity) with depths ranging from 200 to about 400 m. The grid spacing was 100 m, and the window size of 20 was specified for Fig. 6a, b in the 3D Euler routine. The structural indices 3.0 (magnetic) and 2.0

(gravity) of 3D Euler deconvolution have been used worldwide to detect or explore for tanks and drums (or metalliferous bodies) (Yaghoobian et al. 1992; Marchetti and Settini 2011). The known rare metals and gemstone-bearing pegmatite-rich zones (i.e., Gbugbu, Lema, and Bishewa communities) were therefore demarcated on these maps for correlation purposes. Many of these pipe-like and spherical features correlate with the known pegmatite-rich zones thereby confirming the association of structural indices 2.0 and 3.0 (magnetic) and 1.1 and 2.0 (pseudogravity) with mineral-rich areas. However, other undifferentiated

Fig. 6 **a** A typical aeromagnetic Euler solution map for sphere (SI = 3.0). **b** A typical pseudogravity Euler solution map for sphere (SI = 2.0)



areas which are also rich in pegmatite are shown in Figs. 5 and 6, where mining activity is less organized (e.g., west of Bishewa and south of Gbugbu communities).

Conclusions

This research has evaluated the 2D and 3D structures within the pegmatite-rich zones of Lafiagi study area by using geological, aeromagnetic data and pseudogravity transforms. The 2D and 3D structures which are represented by thin prisms with large depth to sphere (magnetic) and ribbon to sphere

(pseudogravity) are found in large quantity in the study area. The structural indices of 2.0 (i.e., vertical or horizontal cylinder model; magnetic) and 1.1 (i.e., pipe and dyke model; pseudogravity) of 3D Euler deconvolution (see Hsu 2002) have been used worldwide to detect or explore for Kimberlite pipe which is well known for hosting large quantity of minerals (diamonds and garnet) and rocks (peridotite and xenoliths) (Paterson et al. 1991; Yaghoobian et al. 1992), while the structural indices 3.0 and 2.0 (i.e., sphere or dipole model) in magnetic and gravity, respectively, have been used worldwide to detect tanks and drums (or metalliferous bodies) (Yaghoobian et al. 1992; Marchetti and Settimi 2011). Many

of these pipe-like (e.g., Fig. 5a, b) and spherical (e.g., Fig. 6a, b) features correlate with the known pegmatite-rich zones thereby confirming the association of structural indices 2.0 and 3.0 (magnetic) and 1.1 and 2.0 (pseudogravity) with mineral-rich areas. However, other undifferentiated areas which are also rich in pegmatite are found in the study area (Figs. 5 and 6) where mining activity is less organized (e.g., west of Bishewa and south of Gbugbu communities). These have not been discovered because the local miners were mainly operating on a “Hit or Miss” manner, and most of the times, these areas are missed out, whereas the application of technology was able to detect them and show a better picture of the subsurface.

References

- Ball E (1980) An example of very consistent brittle deformation over a wide intra-continental area: the late pan African fracture system of the Tuareg and Nigerian shield. *Tectonophysics* 61:363–379
- Baranov V, Naudy H (1964) Numerical calculations of the formula of reduction to magnetic pole. *Geophysics* 29:69–79
- Barbosa VCF, Silva JBC, Medeiros WE (1999) Stability analysis and improvement of structural index estimation in Euler deconvolution. *Geophysics* 64:48–60
- Barbosa VCF, Silva JBC, Medeiros WE (2000) Making Euler deconvolution applicable to small ground magnetic surveys. *J Applied Geophysics* 43(1):55–68
- Black R, Ba H, Ball E, Bertrand JMI, Boullier AM, Caby R, Davison I, Fabre J, Leblanc M, Wright II (1979) *Outline of the Pan-African geology of Andrar des Iforas* (rep. Of Mali). *Geol Rundsch* 68(2): 543–564
- Caby R, Bertrand JMI, Black R (1981) Pan-African ocean closure and continental collision in the Horgar-Iforas segment. In: Kroner A (ed) Central Sahara, in *Precambrian Plate tectonics*. Elsevier, Amsterdam, pp. 407–434
- Davis, K. and Li, Y. (2009). Enhancement of depth estimation techniques with amplitude analysis: Presented at the 2009 International Exposition and Annual SEG Meeting in Houston.
- Garba, A. A. (2011). Geology, geochemistry and rare-metal bearing potentials of pegmatite of Gbugbu, Lema and Bishewa areas of North Central Nigeria. Unpublished Ph.D Thesis. University of Ilorin, Nigeria. 207 p
- Gilbert D, Geldano A (1985) A computer programme to perform transformations of gravimetric and aeromagnetic surveys. *Comput Geosci* 11:553–588
- Hsu SK (2002) Imaging magnetic sources using Euler’s equations. *Geophys Prospect* 50:15–25
- Kogbe CA, Ajaikaye DE, Matheis G (1983) Confirmation of a rift structure along the mid-Niger Valley Nigeria. *J Afr Earth Sc* 1:127–131
- Leblanc M (1981) The late Proterozoic Ophiolites of Bou Azzer (Morocco) evidence for pan-African plate tectonics. In: Kroner (ed) *Precambrian plate tectonics*. Elsevier, Amsterdam, pp. 435–451
- Likkasson OK, Ojo SB (1999) Additional evidence from gravity for a basic intrusion in the middle Niger Basin, Nigeria. *J Min Geol* 35(2): 171–181
- Marchetti M, Settimi A (2011) Integrated geophysical measurements on a test site for detection of buried steel drums. *Ann Geophys* 54(1): 105–114
- Murat C (1972) In: Dessauvage TFJ, Whiteman AJ (eds) *Stratigraphy and paleogeography of the cretaceous and lower tertiary in south-eastern Nigeria*. University of Ibadan Press, African Geology, pp. 251–266
- Obaje NG (2009) Geology and mineral resources of Nigeria. *Lect Notes Earth Sci* 120:13–30
- Ojo, S. B. (1984): Middle Niger Basin revisited, magnetic constraints on gravity interpretations. Abstract 20th Nigeria Min. and Geosci. Soc. Conference, Nsukka, Nigeria, pp. 52–53.
- Ojo SB, Ajakaye DE (1989) Preliminary interpretation of gravity measurement in the middle Niger Basin area of Nigeria. In: Kogbe CA (ed) *Geology of Nigeria*, second edn. Elizabethan Pub. Co., Lagos, pp. 347–358
- Paterson, N. R., Kwan, K.C.H., and Reford, S.W. (1991): Use of Euler deconvolution in recognizing magnetic anomalies of pipelike bodies: extended abstract G/M2.6, p 642–645, SEG Annual Meeting, Houston.
- Reid AB, Thurston JB (2014) The structural index in gravity and magnetic interpretation: errors, uses and abuses. *Geophysics* 79(4):J61–J66. doi:10.1190/GEO2013-0235.1
- Reid AB, Alisop JM, Granser H, Millett AJ, Somerton IW (1990) Magnetic interpretations in three dimensions using Euler deconvolution. *Geophysics* 55:80–91
- Sharma PV (1997) *Environmental and engineering geophysics*. Cambridge University Press, Cambridge, p. 475
- Silva JBC (1986) Reduction to the pole as an inverse problem and its application to low-latitude anomalies. *Geophysics* 51:369–382
- Thompson, D.T. (1973). Identification of magnetic source types using equivalent simple models: Presented at the 1973 Fall Annual AGU Meeting in San Francisco.
- Thompson DT (1982) EULDPH: a new technique for making computer-assisted depth estimates from magnetic data. *Geophysics* 47:31–37
- Whitehead, N. and Musselman C. (2005). *Montaj Grav/Mag Interpretation*. Processing, analysis and visualization system for 3-D inversion of potential field data for Oasis Montaj™, Tutorial and User Guide, Version 6.1, Geosoft Inc. Toronto, ON Canada M5 J 1 A7.
- Wright JB (1976) Origins of the Benue Trough—a critical review. In: Kogbe CA (ed) *Geology of Nigeria*. Elizabethan, Lagos, pp. 309–317
- Yaghoobian, A., Boustead, G.A., and Dobush, T.M.(1992): Object delineation using Euler’s homogeneity equation. Location and Depth Determination of Buried Ferro-Metallic Bodies: Proceedings of SAGEEP 92, San Diego, California.